Thermal Effect on the Oxides Grown on Nb(100)

Q. Ma, P. Ryan, J. W. Freeland, R. A. Rosenberg
Advanced Photon Source, Argonne National Laboratory, Argonne, IL, U.S.A.

Introduction

Next-generation accelerators will employ Nb rf cavities to achieve the highest possible accelerating field. The technology of cavity processing is maturing [1]. Recent experiments show that baking the cavities near 150°C improves cavity performance significantly [2], a result that is yet to be understood. Here we report some results on single crystal Nb surface oxides obtained by using glancing-incidence x-ray photoelectron spectroscopy (GIXPS) and polar angle-resolved x-ray photoelectron spectroscopy (ARXPS).

Methods and Materials

X-ray photoelectron spectroscopy (XPS) experiments were performed at beamline 4-ID-C at APS, which operates in an energy range from 500 to 3000 eV. A spherical grating monochromator was used to select 600-eV photons. The slits were set at 0.1×1 mm^2. Attached to the beamline is (1) an ultrahigh vacuum system (UHV) system that houses an energy analyzer and (2) an X-Y-Z-ϕ manipulator on which the sample is mounted vertically. The base pressure was 5×10^{-10} Torr. The energy resolution δ_{ins} was 540 meV, determined by using the Au *4f* line measured on an Au foil. The sample was annealed at 430 and 540K by using a W filament, and a thermocouple measured surface temperatures. Both core-level and valence band spectra were collected. The binding energies were determined by reference to the Fermi level. The Nb(100) surface was etched by using buffered chemical polishing (BCP) solutions (1:1:1 and 2:1:1 HPO_3:HNO_3:HF) that were cooled down to < 10°C. The polished surface was rinsed alternatively in deionized (DI) water, HNO_3, and HF. Etched surfaces were oxidized in air for a few days.

For large incidence angles ϕ, x-rays penetrate into a solid medium with negligible refraction. When ϕ is small enough, the refraction effect is no longer negligible, and x-ray "total-reflection" occurs at a critical angle ϕ_c. Strong x-ray absorption and resonance effects confine x-ray photons in the near surface region. This effect has been used to develop a host of surface-sensitive techniques, including GIXPS. In the case of GIXPS, the surface sensitivity is further enhanced, since the probing depth depends on both the x-ray incidence angle and the electron detection angle θ; that is, $d_z = 1/(2\gamma + \Lambda)$ [3], where γ = the imaginary part of the wave vector in the depth direction that dominates at small ϕ, and $\Lambda = 1/(\lambda\cos\theta)$, where λ = the photoelectron mean free path. For ARXPS, $d_z = 1/\Lambda$.

Results and Discussion

Figure 1 presents the results of GIXPS compared with those of ARXPS in terms of the ratios of Nb_2O_5 over suboxides plus metal Nb. GIXPS is much more surface-sensitive for $\phi < \phi_c$, for which d_z is only a fraction of λ (= 9 Å at $h\nu$ = 600 eV). When $\phi > \phi_c$ by a few degrees, the polar angle dependence dominates. The insert shows the experimental layout. The surface oxides are identified to be Nb_2O_5, NbO_2, NbO, and Nb_2O from the surface top to the metal substrate. The oxide thickness was determined by photoelectron attenuation as a function of photon energy; i.e., $e^{-t/\lambda}$, where λ = a function of the kinetic energy of the photoelectrons. The thickness measured is ~19 Å for Nb_2O_5 and ~14 Å for suboxides in total.

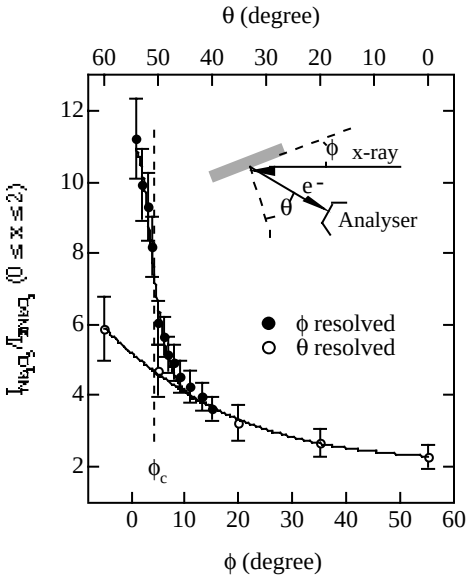

FIG. 1. GIXPS (filled circles) and ARXPS (open circles) results. Insert: Schematic layout.

Figure 2 shows a Nb 3d spectrum (circles) collected at ϕ = 2° and 300K. The line shapes (dots) are analyzed by Doniach-Sujic functions. For Nb_2O_5, the Nb 3d lifetime

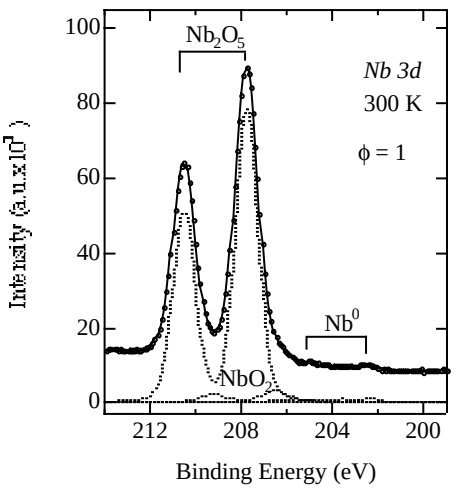

FIG. 2. A Nb 3d spectrum (circles). The solid line and dotted lines are simulation results.

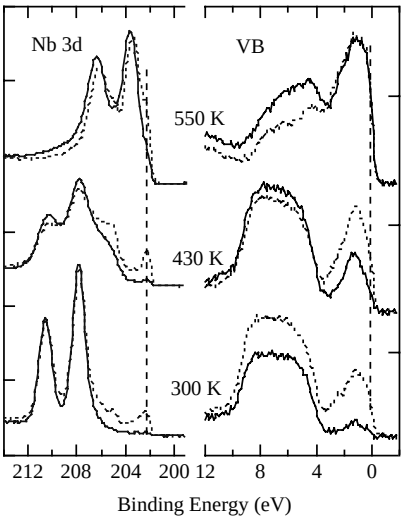

FIG. 3. Nb 3d (left) and valence band (right) spectra collected at ϕ = 2° (full line) and θ = 0° (dashed line) on the surfaces after annealing.

width = 0.2 eV and its Gaussian width δ = 1.05 eV. A spreading of the Nb 3d photoelectrons δ_G = 0.9 eV [= $(\delta^2 - \delta_{ins}^2)^{1/2}$]. The δ_G may result from lattice vibration or from structural fluctuation for a disordered system, where the interatomic distances q fluctuate around a mean value q_0 whose distribution usually is a Gaussian function of $q - q_0$ (= Δq). The XPS measurements carried out as a function of temperature from 300 to 140K indicate no phonon broadening. Therefore, δ_G is structural. In a disordered system, a photoexcitation process will sample the distribution of potential wells about q_0 due to distance variation, which has been appreciated through x-ray absorption or scattering measurements of the Debye-Waller factor [4]. By using a simple harmonic oscillator model [5], δ is related to the relaxation energy ΔE by $2(2\ln 2)^{1/2}(\hbar\omega_0\Delta E)^{1/2}$ multiplied by a temperature factor, where $\Delta E = M(v_0\Delta q)^2/2$, in which M = the reduced mass and v_0 (= $\omega_0/2\pi$) = the vibration frequency (= 10^{13} s^{-1} at T = 300K). An averaged Δq is obtained and considered to be 0.06 , which leads to $T/\Theta > 140$ [6], where Θ is the Debye temperature, implying a liquidlike structure (i.e., an amorphous phase in this case).

At 300K, GIXPS unequivocally indicates that NbO_2 exists *predominantly* as a suboxide under the Nb_2O_5 layer, rather than point defects in the Nb_2O_5 matrix (oxygen vacancies) [7], and that upon annealing, the chemical reaction (namely reduction of Nb_2O_5) occurs *primarily* at the interface between NbO_2 and Nb_2O_5. Figure 3 shows the Nb 3d and valence band spectra collected at ϕ = 2 and θ = 0 for 300K, 30-h annealing at 430K, and further 8-h annealing at 550K. Changes in the core-level and valence band spectra appear to be similar.

At 430K, the reaction proceeds until the significant amount of Nb_2O_5 has reduced to NbO_x ($1.5 \le x \le 2$). At 550K, the reaction stops when Nb_xO (x ~2) dominates the oxide layer. The valence band consists of Nb 4d orbitals and O 2p origin. The density of states (DOS) *localized* around 1.2 eV in the band gap of Nb_2O_5 is associated with a Nb^{4+} entity; the bulk NbO_2 is a semiconductor at T < 1100K [8]. This assignment is also supported by a large increase of this DOS by annealing at 430K that produces more NbO_2 at the interface as well as some Nb_2O_3. Therefore, annealing produced a layer of semiconductor that is sandwiched by an insulator and a metal [9, 10]. For such a structure, the *overlap* of the DOSs at interfaces could have important consequences on superconductor interaction with the oxides [11]. By further annealing at 550K, the oxide consists primarily of Nb_xO (x ~2) (see Fig. 3). The shift of the Nb_xO peak seen for the ϕ = 2 and θ = 0 data shows that this peak does not contain a single well-defined oxide (e.g., Nb_2O) but rather oxides with a compositional gradient $\partial x/\partial d$ that changes rapidly near the oxide surface from x = 2 to 0.4. This compositional *continuity* across the oxide is clearly reflected in the valence band, which has filled the minimum existing originally between the O 2p and Nb 3d bands. The 550K annealed surface is metallic, and its valence band does indicate an *apparent* de-localization character.

Both the band gaps ΔE and work functions W of polymorphic Nb_2O_5 phases are $\ge$ and > 3.5 eV [12], respectively, suggesting that they should be stable when subjected to heating at moderately high

temperatures (e.g., $\leq$ 550K). However, Nb_2O_5 is destabilized at the interface (to the suboxides), which provides a channel for chemical reaction to occur by effectively reducing the band gap or increasing *d-p* state interaction. The activation energy is only ~1 eV in the case of polycrystalline Nb [13]. Therefore, the chemical reaction is *interface* mediated. The reaction at 430K is *essentially* contained in the oxide layer, with oxidation of the suboxides adjacent to the metal substrate. The higher temperature facilitates the oxygen diffusion into the Nb metal that has a higher density; the probability for oxygen to diffuse into vacuum, $e^{-(W+\Delta E)/kT}$, is ~ 0.

The metal Nb 3d peak is better defined upon annealing at 420K because of the desorption of loosely bound species on the surface, as indicated by the detailed analysis of Nb 3d and O 1s spectra as a function of annealing. It is thus clear that the chemical reaction at 430K may be written categorically as follows:

$$2\,Nb_2O_5 \xrightarrow{\Delta} 2NbO_2 + Nb_2O_3 + \frac{3}{2}O_2 \ .$$

For annealing at 550K, the reaction is predominantly as follows:

$$Nb_2O_5 \xrightarrow{\Delta} Nb_2O + 2O_2 \quad \text{and}$$

$$Nb + O_2 \xrightarrow{\Delta} NbO_x \ .$$

The total thickness of the oxide after annealing at 550K is about 30 Å, which is only slightly smaller than the thickness before heat treatment. Both oxide surfaces obtained by annealing are stable in ultrahigh vacuum and have lower secondary electron yields (~1.4 once annealed at 430K and ~1.2 once annealed at 550K) than the as-oxidized surface (~1.8 at 300K).

The ARXPS measurements on the 550K annealed surface indicate that around $\theta = \pm 20°$, the photoelectron intensity originated from the substrate is enhanced significantly. Preliminary analysis suggests that this enhancement is likely a result of the photoelectron diffraction through an ordered oxide phase. Therefore, annealing at 550K has produced a crystalline oxide layer on the Nb surface. By using low-energy electron diffraction (LEED), Farrell et al. reported that a facetted, crystalline oxide layer formed on the Nb surface when oxidized by exposure to 10^{-4} Torr oxygen at temperatures from 773 to 1273K [14, 15]. The oxide was described as NbO and as being in the form of nodules on the substrate. The fact that the observed photoelectron diffraction is symmetrical about the Nb(100) axis may indicate that the crystalline oxide layer is also faceted, but its composition is mainly Nb_2O.

GIXPS and ARXPS are used to study the oxide layer on the Nb (100) surface. The results show that the predominant Nb_2O_5 oxide layer, grown in air at room temperature after the BCP treatment, is amorphous and that NbO_2 exists mainly as a suboxide at the interface instead of point defects in the Nb_2O_5 matrix (oxygen vacancies), as speculated previously [7]. The experimental results also show that upon thermal annealing, the reduction of Nb_2O_5 is driven by the reaction at the interface where the DOS of NbO_2 is pinpointed to lie in the band gap of Nb_2O_5. Annealing at 430K produces an oxide layer that is much less "abruptly" interfaced with the metal, in terms of both composition and possibly physical properties. Annealing at 550K produces an oxide layer that consists predominantly of metallic, crystalline Nb_2O with some Nb_xO on the surface where x changes rapidly from 2.0 to 0.4. It is likely that this crystalline oxide layer is also faceted.

Acknowledgments

Use of the APS was supported by the U.S. Department of Energy, Office of Science, Office of Basic Energy Sciences, under Contract No. W-31-109-ENG-38.

References

[1] H. Padamsee, J. Knobloch, and T. Hays, *RF Superconductivity for Accelerators* (John Wiley & Sons, Inc., New York, NY, 1998).
[2] P. Kneisel, in *Proc. of the 9th Workshop on RF Superconductivity* (Santa Fe, NM, 1999), p. 328.
[3] M. J. Chester and T. Jach, Phys. Rev. B **48**, 17262 (1993).
[4] Q. Ma, D. Rouax, and S. Benazeth, Phys. Rev. B **48**, 16332 (1993).
[5] P. H. Citrin and D. R. Hamann, Phys. Rev. B **15**, 2923 (1977).
[6] J. M. Zimman, *Principles of the Theory of Solids* (Cambridge University Press, Cambridge, 1972).
[7] J. Halbritter, Appl. Phys. A **43**, 1 (1987).
[8] G. Thornton, A. F. Orchard, and C. N. R. Rao, Phys. Lett. A **54**, 235 (1975).
[9] R. Sanjinés, H. Tang, H. Berger, F. Gozzo, G. Margaritomdo, and F. Lévy, J. Appl. Phys. **75**, 2945 (1994).
[10] R. L. Kurtz and V. E. Henrich, Phys. Rev. B **28**, 6699 (1983).
[11] J. Halbritter, Solid State Commun. **34**, 675 (1980).
[12] I. Lindau and W. E. Spicer, J. Appl. Phys. **45**, 3720 (1974).
[13] B. R. King, H. C. Patel, D. A. Gulino, and B. J. Tatarchuk, Thin Solid Films **192**, 351 (1990).
[14] H. H. Farrell and M. Strongin, Surf. Sci. **38**, 18 (1973).
[15] J. M. Dickey, H. H. Farrell, O. F. Kammerer, and M. Strongin, Phys. Lett. A **32**, 483 (1970)